[Chem. Pharm. Bull. 33(5)1782—1792(1985)]

Differential Scanning Calorimetry Study of Polymorphism in Cholesteryl Oleate

HIROSHI KISHIMOTO,* TAKAO IWASAKI, and MASAKATSU YONESE

Faculty of Pharmaceutical Sciences, Nagoya City University, Tanabe-dori, Mizuho-ku, Nagoya 467, Japan

(Received July 31, 1984)

The phase transitions among various phases, *i.e.* crystalline (k), isotropic liquid (i), cholesteric (c) and smectic (s) phases, of cholesteryl oleate (ChO) were studied by using differential scanning calorimetry (DSC) and polarizing microscopy. We used two commercial samples of ChO and a gift with a known history of synthesis and purification. The transition temperatures, T_{tr}, and enthalpies, $\Delta_{tr}H$, of these samples were all in good agreement with each other. The DSC thermograms of k/i transition showed the coexistence of two kinds of crystals with a higher melting temperature (k_1) and a lower one (k_2) in k. By analysis of the thermograms, we determined the enthalpic and molar fractions of k_1 in k, f_1 and x_1, respectively, which depend on the method and conditions of crystallization. Three types of crystallizing procedures, *i.e.* solvent evaporation, cooling of ChO solution in ethanol, acetone or 1-pentanol, and *in situ* crystallization in the DSC pan, were examined at various temperatures. At higher temperature, a higher value of f_1 or x_1 was obtained. Using the values of T_{tr} and $\Delta_{tr}H$ at various transitions, we could draw the curves of relative chemical potential, μ_{rel}, of the k_1, k_2, i, c and s phases of ChO *vs.* temperature. The stability of various ChO phases and the thermodynamic nature of the transition paths are discussed on the basis of the above μ_{rel} diagram.

Keywords——cholesteryl oleate; DSC; liquid crystal; mesophase; chemical potential; phase transition; enthalpy; polymorphism

Introduction

Esters of cholesterol with various fatty acids are known to have two *meso*-phases (or liquid crystals), *i.e.* smectic and cholesteric phases (s and c, respectively), as well as normal crystalline and isotropic liquid phases (k and i).[1] Such a polymorphism of cholesteryl esters is of interest to scientists working in medicinal and biological fields, because of the significance of liquid crystals in living systems, such as in biomembranes.[2b] For this reason, and also because of the solubilizing behavior of mesogenic[1] (or liquid-crystal-forming) cholesteryl esters *in vivo*, we have studied thermodynamically as well as viscometrically the interactions between them and non-mesogenic organic compounds.[3-6] However, in order to understand the results, it is necessary to clarify the dynamic behavior of cholesteryl esters at the molecular level. Thus, we are examining the esters by measuring their nuclear magnetic resonance (NMR) chemical shifts and relaxations. As initial samples for NMR measurements, we chose cholesteryl oleate (ChO) and linoleate (ChL), both of which exhibit all the kinds of phases, *i.e.* k, s, c and i in the range of temperature where NMR as well as other usual physico-chemical measurements can be made without difficulty and the living system can function normally. Although several authors[4,7-9] have reported on the basic characteristics of ChO and ChL, *i.e.* temperatures and enthalpies of transitions between various phases, there are significant disagreements among the results, especially with respect to the k/i transition of ChO, and also, there is ambiguity concerning the conditions of crystallization before measurements. We scrutinized the thermal behavior of ChO from various sources by differential scanning

calorimetry (DSC) and polarizing microscopy (PM), as follows.

Experimental

Materials——We used three kinds of ChO, *i.e.* two commercial samples from Tokyo Chem. Ind. Co. and Sigma Chem. Co., and a sample provided together with information on its synthesis and purification by the Research Laboratory of Nippon Oil & Fats Co. (R.N.O.). These samples are abbreviated as ChO-T, ChO-S, and ChO-N, respectively. As the original lot of ChO-T was found to contain impurities such as cholesterol by inspection of its thin-layer chromatogram, it was recrystallized twice from ethanol and then twice from 1-pentanol for purification,[7] dried *in vacuo* at room temperature for several days and stored in a nitrogen-filled container at *ca.* 275 K before use. ChO-S (Sigma grade, crystals) was used without further purification; it was stored under conditions similar to those used for ChO-T. The synthesis and purification of ChO-N were carried out by the donor (R.N.O.), as follows: ChO-N was prepared by the reaction of oleyl chloride with cholesterol (Katayama Chem. Inc. Co., Ltd. (K.C.I.), JIS. first reagent grade, recrystallized from acetone) in toluene, purified by column chromatography on Kieselgel 60 (E. Merck, Darmstadt) with benzene/*n*-hexane (1 : 1) and crystallized in a vacuum evaporator. The above-mentioned oleyl chloride and its precursor, olein, were also synthesized by R.N.O. Of them, olein was prepared through biosynthesis in order to exclude the *trans*-isomer and double-bond position isomers, which are found at the level of a few percent in natural oils. Therefore, ChO-N can be considered to consist of pure cholest-5-en-3β-ol(*Z*)-9-octadecenoate. ChO-N, thus obtained, was dried further *in vacuo* and stored by us under the same conditions as ChO-T and ChO-S.

Naphthalene from K.C.I. (G.R.) and benzophenone and *p*-nitrotoluene from Waco Pure Chem. Ind., Ltd. (G.R.) were used for DSC calibration after recrystallization from ethanol. Deionized and twice distilled water was also used for DSC calibration. Ethanol and 1-pentanol from K.C.I. (G.R.) were twice distilled before use.

Apparatus and Procedures——The following instruments were used for the chemical assay of ChO by infrared spectra (IR), NMR and elemental analyses: IRA-2, Japan Spectroscopic Co.; FX-100/MH-100, Japan Electron Optics Laboratory Co.; MT-3, Yanaco Ltd., respectively. The thin-layer chromatography (TLC) of ChO was performed on Silica gel G (Analtech) using benzene/*n*-hexane (1 : 1) as the eluent and I_2 as the developer.

DSC: To study the thermal behavior of ChO, we used a differential scanning calorimeter (Seiko Instruments & Electronics Ltd., SSC 560U), or strictly speaking, a quantitative differential thermal analyzer, which, however, serves as a precise substitute for DSC if a small quantity of sample is used. Usually, *ca.* 5 mg of ChO crystalline sample was weighed in an aluminum sample pan. The error of enthalpy in a single DSC measurement arising from the weighing of the sample is at most one percent. After being sealed with an aluminum lid, the pan was set in the calorimeter, together with another vacant pan as a reference. During the normal DSC scan, the heating rate and output sensitivity of the calorimeter were *ca.* 0.5 K min^{-1} and 0.5 mV s^{-1} mJ^{-1}, respectively. Using water, benzophenone, *p*-nitrotoluene and naphthalene as standards, the calorimeter was calibrated with respect to temperature and heat over the temperature range from 273 to 353 K.[10] For the calibration of temperature, we regarded the extrapolation of the DSC curve to the onset of phase transition as corresponding to the thermodynamic transition temperature of pure standard material. Therefore, we regard the extrapolation or the onset temperature of the DSC phase transition peak for ChO as its formal transition temperature. However, we also determined the so-called peak temperature for the sake of comparison with the results of other workers who used the latter as the characteristic temperature of liquid crystalline materials. The transition enthalpy of a DSC sample (standard or ChO) was determined as the area enclosed by the heat inflow, $\dot{q}$, *vs.* time curve under the transition peak and the line connecting the base-lines before and after the peak. The k/i transition temperatures and enthalpies of reference materials used for DSC calibration are shown in Table I.

PM: Transition characteristics of ChO were observed[11] using a polarizing microscope (Olympus Optical Co., model POS) with a hot stage (Mettler Instrumente A.G., model FP5, FP52) between crossed polarizers. A standard white light source (Nippon Kogaku K.K., 6 V, 30 W tungsten lamp) was used. Usually 3—5 mg of sample was examined at the heating and cooling rate of 2 K min^{-1}

TABLE I. The k/i Transition Temperatures and Enthalpies of Reference Materials for DSC

Material	Water[a]	Benzophenone[a]	*p*-Nitrotoluene[b]	Naphthalene[a]
T_{tr}/K	273.15	321.41	324.85	353.41
$\Delta_{tr}H$/kJ·mol^{-1}	6.0	17.9	17.0	18.8

a) and *b*) See references 10*a*) and 10*b*), respectively.

Results and Discussion

Chemical Assay of ChO

Anal. Calcd for $C_{45}H_{78}O_2$: C, 83.01; H, 12.07; O, 4.92. Found (mean of three samples; the value for O was estimated as 100 minus the sum of the values for C, H and N, assuming the absence of any other element in smaples): [ChO-T] C, 82.85; H, 12.26; N, 0.06; O, 4.83. [ChO-S] C, 82.99; H, 12.31; N, 0.04; O, 4.66. [ChO-N] C, 82.89; H, 12.33; N, 0.09; O, 4.69. The results of elemental analysis showed no appreciable difference among ChO-T, ChO-S, and ChO-N. Further, the ^{1}H- and ^{13}C-NMR spectra in chloroform-d_1 (E. Merck, Darmstadt; NMR spectroscopic grade) as well as the IR spectra in carbon tetrachloride (K.C.I., S.G.) coincided well among the three kinds of samples. Therefore, it may be concluded that the samples are chemically identical with each other and contain no detectable impurities. (This was confirmed qualitatively by TLC.)

Transfer Scheme for ChO

The thermotropic transition paths of ChO found by DSC and PM were qualitatively common to all samples and agreed with the results of other workers.[7,8] On heating after retention at room temperature for half an hour or so, ChO undergoes the k/i transition at about 320 K, usually with two peaks on the DSC thermogram, as shown in Fig. 1(a). The transition is considered to be a kind of monotropy, since the reverse i/k transition cannot be observed during the simple cooling of i, probably due to the difficulty of nucleation of k in i. However, in the *in situ* crystallization in a DSC pan, which will be described later, we could observe the exothermic process of i/k transition by cooling ChO before the complete disappearance of k in the course of k/i transition on heating in DSC. Thus, the k/i transition process is reversible from the thermodynamic standpoint, which justifies the following equation for the isobaric transition.

$$\Delta_{tr}S = \Delta_{tr}H/T_{tr} \tag{1}$$

where $\Delta_{tr}S$, $\Delta_{tr}H$ and T_{tr} are the transition entropy, enthalpy, and temperature, respectively. As already mentioned, the k/i transition has two DSC peaks, which suggest the coexistence of two kinds of ChO crystalline phases, designated hereafter as k_1 and k_2, in place of k, with higher and lower transition temperatures respectively. Under suitable conditions, which will be discussed later, we can obtain ChO crystals in which either k_1 or k_2 is dominant, resulting in almost a single DSC peak for the transition to i, as can be seen in Fig. 1(b) and (c).

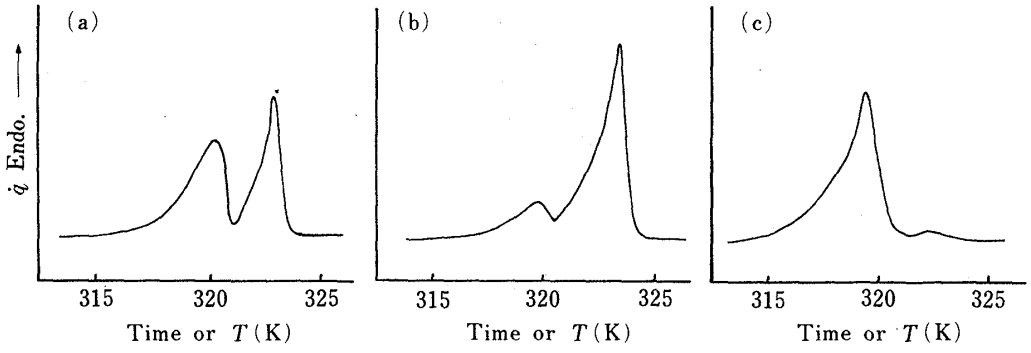

Fig. 1. DSC k/i Transition Thermograms of the Cholesteryl Oleates Recrystallized under Various Conditions

Ordinate: heat inflow per unit time, $\dot{q}$. Abscissa: time or the corresponding temperature scale (T/K).
(a) ChO-T crystallized at 298 K from a supersaturated solution in 1-pentanol. (b) ChO-T crystallized at 318 K by gentle solvent evaporation from 1-pentanol. (c) ChO-T crystallized at 253 K by rapid cooling from 1-pentanol.

TABLE II. Transition Temperatures and Enthalpies of Various Cholesteryl Oleates

Transition		Substance				
		ChO-T	ChO-S	ChO-N	ChO[a]	ChO[b]
k_1/i	$\frac{T_{tr}}{K}$	321.15 (322.85)[c]	321.65 (322.65)	319.75 (321.15)	(323.75)	(321.50)
	$\frac{\Delta_{tr}H}{kJ \cdot mol^{-1}}$	29.0[d] ± 0.24[e]	31.2[d] ± 0.88[e]	31.4[d] ± 0.80[e]	30.6	28.7
k_2/i	$\frac{T_{tr}}{K}$	317.35 (320.35)	319.45 (320.75)	318.25 (320.25)	(322.25)	(320.00)
	$\frac{\Delta_{tr}H}{kJ \cdot mol^{-1}}$	27.0[d] ± 0.24[e]	27.0[d] ± 0.88[e]	27.2[d] ± 0.80[e]	28.9	21.8
c/i	$\frac{T_{tr}}{K}$	321.0 (321.35)	318.65 (318.95)	317.65 (318.15)	(318.25)	(318.30)
	$\frac{\Delta_{tr}H}{kJ \cdot mol^{-1}}$	0.84[f] ± 0.025[e]	0.79[f] ± 0.065[e]	0.58[f] ± 0.0087[e]	0.68	0.57
s/c	$\frac{T_{tr}}{K}$	315.85 (316.25)	313.25 (313.75)	312.35 (312.65)	(312.40)	(312.40)
	$\frac{\Delta_{tr}H}{kJ \cdot mol^{-1}}$	1.26[f] ± 0.043[e]	1.22[f] ± 0.062[e]	1.00[f] ± 0.015[e]	1.53	0.93

a) Sample used by Porter and Krzewki.[7] *b*) Sample used by Armitage.[8] *c*) The values in parentheses denote the peak temperature in DSC thermogram. See the text. *d*) Extrapolated value. See the text. *e*) Standard deviation of extrapolated or mean value. *f*) Mean value.

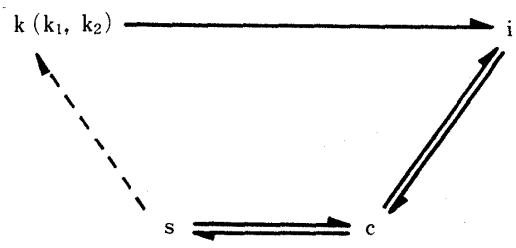

Chart 1. The Phase Transition Diagram of Cholesteryl Oleate

k_1, crystal with higher melting temperature; k_2, crystal with lower melting temperature; k, collective symbol for crystal phases k_1 and k_2; i, isotropic liquid phase; c, cholesteric phase; s, smectic phase. Arrows with solid shafts denote reversible phase transitions. The broken arrow denotes an irreversible transition accompanied by supercooling. Arrow-heads denote heating or cooling when directed to the right or left, respectively.

On cooling, ChO transforms from i to c to s, and on reheating, it transforms from s to c to i at the same transition temperatures as seen on cooling. Therefore, the s/c and c/i transitions of ChO are both thermodynamically reversible procedures. In comparison with the case of the monotropic k/i transition, they are regarded as enantiotropic.

On further cooling from s, ChO undergoes a transition to the mixture of k_1 and k_2, giving an exothermic DSC thermogram similar to the contour of $(k_1+k_2)/i$, as shown in Fig. 1(a), but more lumpy and sometimes with more than two peaks. The transition temperature lies around 300 K, scattering in each DSC run with poor reproducibility. On the basis of the above result and the later discussion on the chemical potential of ChO *vs.* temperature relationship (Fig. 4), the transition is considered to be as thermodynamically irreversible process.

On the basis of the thermotropic behaviors of ChO-T, -S and -N, we may summarize the

transition paths at temperatures above room temperature as shown in Chart 1 and Table II. The latter includes the results of other workers,[7,8] as well as the transition enthalpies from DSC. There are fairly good agreements among the different samples of ChO with respect to various transition temperatures and enthalpies, except that the c/i and s/c transition temperatures of ChO-T are slightly higher than those of the other samples and the k_2/i transition enthalpy reported by Armitage[8] is lower than those found by us and by Porter and Krzewki.[7] These differences will be discussed later. The diffference of the c/i or s/c transition enthalpies among samples is considered to be negligible, at least in this work, in view of their small absolute values.

Fraction of k_1 or k_2 Phase in ChO Crystals

First, we assume that the k_1 and k_2 phases in ChO crystals melt independently of each other to an isotropic phase, when the DSC thermogram exhibits a k/i transition with two peaks, as shown in Fig. 1(a). Then, the overall k/i transition enthalpy, $\Delta^{i}_{k}H$, or that divided by the amount of ChO, n, *i.e.* the mean molar transition enthalpy, ΔH_m, can be expressed as the sum of two contributions from the k_1 and k_2 phases. Thus,

$$\Delta^{i}_{k}H = n_1\Delta H_1 + n_2\Delta H_2 \tag{2}$$

or

$$\Delta H_m = x_1\Delta H_1 + x_2\Delta H_2 \tag{3}$$

where n_1, x_1 and ΔH_1 are the amount, mole fraction and molar enthalpy of ChO in the k_1 phase, respectively, and n_2, x_2, and ΔH_2 are the counterparts in the k_2 phase. Clearly,

$$n = n_1 + n_2, \quad \text{and} \quad x_1 + x_2 = 1 \tag{4}$$

Here, we define the enthalpic fraction of k_1 phase in ChO, f_1, as the first term divided by the sum of the first and second terms in Eq. 2 or Eq. 3, as follows.

$$f_1 = n_1\Delta H_1/(n_1\Delta H_1 + n_2\Delta H_2) = x_1\Delta H_1/(x_1\Delta H_1 + x_2\Delta H_2) \tag{5}$$

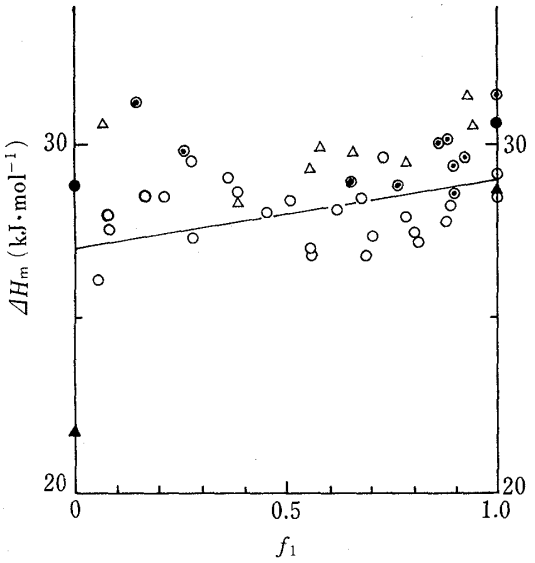

Fig. 2. The Mean Molar k/i Transition Enthalpy, ΔH_m, Plotted against the Enthalpic Fraction of k_1 Phase, f_1, in Cholesteryl Oleates Crystallized under Various Conditions

○, ChO-T; △, ChO-S; ⊙, ChO-N; ▲, values reported by Armitage;[8] ●, values reported by Porter and Krzewki.[7]

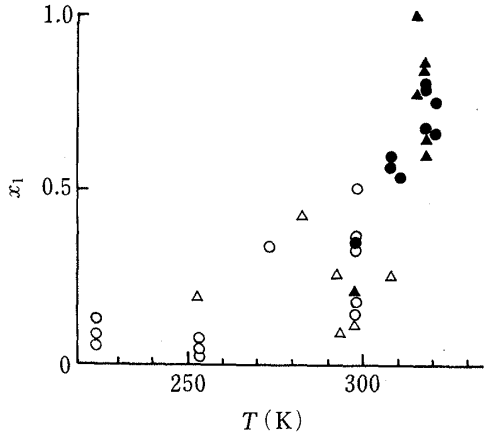

Fig. 3. The Molar Fraction of k_1 Phase, x_1, in ChO-T Plotted against the Temperature, T, at Which Crystallization was Performed

Solvent: 1-pentanol (circles) or acetone (triangles). Recrystallization method: cooling (open symbols) or solvent evaporation (closed symbols).

Similarly, we can define f_2 for the k_2 phase. The f_1 or f_2 is the quantity which can be directly obtained from DSC as the area under the k_1 or k_2 peak divided by that under the whole k/i transition $\dot{q}$ *vs.* time curve over the base-line. The division was performed by drawing on the DSC thermogram the two contours estimated approximately as the curves corresponding to the k_1 and k_2 phases, independent of each other. The estimation of contours was done by selecting as references DSC thermograms which have single peaks for k_1 or k_2 as far as possible. It is considered that ambiguity in dividing the area of the thermogram should not amount to more than a few percent.

As will be described below, the fraction of k_1 or k_2 phase in a ChO sample depends upon the conditions of crystallization. The ΔH_m of ChO samples obtained under various conditions of crystallization are plotted against f_1 in Fig. 2, showing a slight variation of ΔH_m, which depends upon f_1, or suggesting inequality between ΔH_1 and ΔH_2. Taking into consideration the error of ΔH_m in a single DSC measurement, we found an approximately linear relationship between ΔH_m and f_1 for ChO-T. A similar tendency seems to exist for ChO-S and ChO-N, although the number of DSC plots is insufficient. We may then determine ΔH_1 and ΔH_2 and convert f_1 to x_1 as follows.

From the combination of Eq. 3 and Eq. 5, we have

$$\Delta H_m = \Delta H_1 \Delta H_2 / \{\Delta H_1 - f_1(\Delta H_1 - \Delta H_2)\} \tag{6}$$

Differentiation of Eq. 6 with respect to f_1 yields the slope of ΔH_m *vs.* f_1, *i.e.*

$$d\Delta H_m/df_1 = \Delta H_1 \Delta H_2 (\Delta H_1 - \Delta H_2)/\{\Delta H_1 - f_1(\Delta H_1 - \Delta H_2)\}^2 \tag{7}$$

When the difference, $\Delta H_1 - \Delta H_2$, is small compared to the value of ΔH_1 or ΔH_2, the slope given by Eq. 7 becomes nearly constant, resulting in linearity of the ΔH_m *vs.* f_1 relationship, which seems the case for ChO-T in Fig. 2. In the limit when f_1 approaches 0 or 1, the slope becomes constant, *i.e.* $\Delta H_2(\Delta H_1 - \Delta H_2)/\Delta H_1$ or $\Delta H_1(\Delta H_1 - \Delta H_2)/\Delta H_2$, and the value of ΔH_m becomes ΔH_1 or ΔH_2, regardless of the difference between ΔH_1 and ΔH_2. Therefore, the value of ΔH_1 or ΔH_2 can be estimated by drawing a line through the plots of ΔH_m *vs.* f_1 in the neighborhood of $f_1 = 0$ or 1 and reading the intercept with the ordinate, even if $\Delta H_1 - \Delta H_2$ is not negligible. In our case for ChO-T, we estimated the values of ΔH_1 and ΔH_2 from the line drawn through all the plots of ΔH_m *vs.* f_1 between $f_1 = 0$ and 1, taking into consideration their scattering. For ChO-S and ChO-N, where fewer plots were available, we roughly estimated both values. As can be seen in Table II, the values for ChO-S are the closest to those obtained by Porter and Krzewki.[7]

Substituting f_1 as well as ΔH_1 and ΔH_2 into the following equation obtained by the combination of Eq. 4 and Eq. 5, we can convert f_1 to x_1.

$$x_1 = f_1 \Delta H_2 / \{\Delta H_1 - f_1(\Delta H_1 - \Delta H_2)\} \tag{8}$$

Difference of Crystalline Polymorph Content among Samples

First, we measured the f_1 values from DSC thermograms of the ChO samples from different sources and after calculation according to Eq. 8, found the difference of x_1 among samples, as shown in the first row of Table III. Taking into consideration the possible difference of crystallizing conditions among samples, we crystallized ChO from an unsaturated dilute solution at 298 K in a thermostated desiccator by mildly evaporating the solvent under slightly reduced pressure. The solvents used were ethanol, acetone and 1-pentanol (K.C.I., G.R., distilled); the solubilities of ChO at 298 K are *ca.* 0.05, 0.8 and 8.2×10^{-3} (mole fraction), respectively. The results of crystallization by solvent evaporation for various ChO samples are shown in Table III.

Compared to ethanol, which was the poorest solvent used, acetone and 1-pentanol yielded k_1-rich ChO crystals, except in the case of ChO-T. As will be shown later, in terms of

TABLE III. The Enthalpic and Molar Fractions, f_1 and x_1, of Cholesteryl Oleate Crystals Obtained by Solvent Evaporation

Solvent	Sample					
	ChO-T		ChO-N		ChO-S	
	f_1	x_1	f_1	x_1	f_1	x_1
Original[a]	0.43	0.41	0.90	0.89	0.95	0.95
Ethanol	0.38	0.36	0.40	0.38	0.33	0.31
Acetone	0.21	0.20	0.88	0.87	0.89	0.88
1-Pentanol	0.40	0.38	0.75	0.74	0.80	0.79

a) The original sample before recrystallization by solvent evaporation at 298 K.

chemical potential, ChO is thermodynamically more stable in the k_1 phase than in the k_2 phase. Therefore, the abundant presence of the k_2 phase in ChO crystalline samples, especially those produced near room temperature, suggests a lower kinetic barrier in the formation of the k_2 nucleus from ethanol, as compared with k_1. In acetone and 1-pentanol, the kinetic effect seems to be reduced. The low x_1 in ChO-T may be attributed to a trace amount of isomeric impurity, which cannot be easily removed or detected, but which may kinetically facilitate the k_2 formation.

Effect of the Variation of Crystallizing Conditions on x_1

Taking into consideration the small difference of x_1 among solvents and the relatively large amount of sample available, we used ChO-T to examine the effect of temperature and crystallizing conditions on x_1, as follows. Using acetone and 1-pentanol as solvents, we crystallized ChO-T from an unsaturated solution by solvent evaporation, as described above, at various temperatures. The results are shown in Fig. 3. The value of x_1 increases with increase of the temperature and *vice versa*. Near the k/i transition temperature, x_1 approaches its maximum, *i.e.* unity.

On the other hand, we recrystallized ChO-T from a supersaturated solution in acetone or 1-pentanol by cooling to lower temperatures than those adopted for the solvent evaporation method. With the latter method, the "cooling recrystallization" method, essentially the same results were obtained near room temperature, as shown in Fig. 3. Below room temperature, ChO seems to crystallize preferentially in the k_2 phase.

Relative Chemical Potentials of ChO in Various Phases

The thermodynamic stability of ChO in any phase can be compared to that in other phases on the basis of the molar Gibbs energy or chemical potential of ChO. Although the absolute chemical potential cannot be obtained because of the lack of necessary thermodynamic information, we could draw a diagram of relative chemical potential of ChO *vs.* temperature, which indicates the relative stabilities of the phases at various temperatures and explains the transition paths of ChO, which are peculiar to a mesogenic compound. Thus, we obtained a concrete and quantitative example of the thermodynamic treatment which had been proposed by Van Hecke for thermotropic liquid crystals.[12]

The chemical potential of ChO in any phase, μ, varies at constant pressure, according to Eq. 9.

$$\mu=\mu_o-s_o(T-T_o)-\int_{T_o}^{T}\int_{T_o}^{T} C_p \,\mathrm{d}\ln T\,\mathrm{d}T \qquad (9)$$

where μ_o and s_o are the chemical potential and molar entropy of ChO at an arbitrary reference

temperature, T_o, respectively, and C_p is the molar heat capacity of ChO. Following the mathematical custom for simplicity, we adopt in the r.h.s. second term of Eq. 9 the same symbol T for variables which denote generically the temperature, but are different in meaning from each other. As T_o, we adopted 300 K, which is near the lowest temperature at which we examined the DSC thermograms of ChO. With the approximation that the value of C_p is constant within a narrow range of temperature, we obtain Eq. 10 by integration of Eq. 9 from T_o to T.

$$\mu=\mu_o-s_o(T-T_o)+C_p(T-T_o)-C_pT\ln(T/T_o) \tag{10}$$

Since the determination of μ_o and s_o in Eq. 10 is not easy, we subtracted the terms containing μ_o and s_o for the k_1 phase, μ_o^1 and s_o^1, respectively, from μ and defined the relative chemical potential of ChO as follows.

$$\mu_{rel}\equiv\mu-\mu_o^1+s_o^1(T-T_o) \tag{11}$$

or

$$\mu_{rel}\equiv C_p(T-T_o)-C_pT\ln(T/T_o) \tag{12}$$

Although the adoption of the k_1 phase as a reference in Eq. 11 is arbitrary, it seems to be a good choice because the value of μ or μ_{rel} of the k_1 phase is found to be the lowest among the phases, as can be seen in Fig. 4, which is drawn from the following analysis of DSC thermograms.

First, substituting into Eq. 12 the value of C_p for the k_1 phase, *ca.* 1.23 kJ K^{-1} mol^{-1}, which was measured by us using a DSC calorimeter, we have the μ_{rel} *vs.* T curve for the k_1 phase (Fig. 4). The thermodynamic parameters, which are used above and hereafter, are those of ChO-T, unless otherwise mentioned. Therefore, the curves plotted in Fig. 4 are for ChO-T.

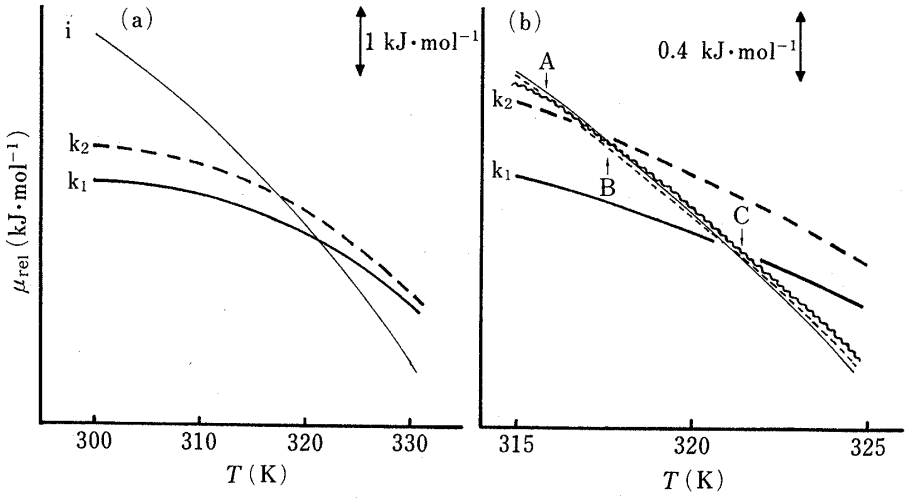

Fig. 4. The Relative Chemical Potential, μ_{rel}, of ChO-T in Various Phases *vs.* Temperature, T

(a) Solid curve, k_1 phase; broken curve, k_2 phase; thin solid curve, i phase. Curves for the s and c phases are omitted. (b) Magnification of (a) in the neighborhood of the k_2/i and k_1/i transition regions. Curves for k_1, k_2 and i phases are the same as in (a). Thin wavy curve, s phase; thin broken curve, c phase. The downward sequence of s, c and i in μ_{rel} are: at temperatures below A, i, c, s; at A (s/c transition temperature), i, s=c; between A and B, i. s, c; at B (s/i transition temperature, not observed), s=i, c; between B and C, s, i, c; at C (c/i transition temperature), s, c=i; at temperatures above C, s, c, i. The k_1/i transition temperature exists at a temperature above C. The k_2/i transition temperature of ChO-T exists near B, probably between A and B, although the position of B cannot be exactly determined owing to the absence of a clear s/i transition in DSC. The k_2/i transition temperature of other samples exists at a temperature above C. Refer to Table II.

Next, in order to plot the μ_{rel} *vs.* T curves for other ChO phases, we modified Eq. 10 to express μ at any arbitrary temperature, T, for two phases of ChO, say α and β phases, which transform into each other at the transition temperature, T_{tr}. We have

$$\mu^{\alpha}=\mu^{\alpha}_{tr}-s^{\alpha}_{tr}(T-T_{tr})+C^{\alpha}_{p}(T-T_{tr})-C^{\alpha}_{p}T\ln(T/T_{tr}) \tag{13}$$

and

$$\mu^{\beta}=\mu^{\beta}_{tr}-s^{\beta}_{tr}(T-T_{tr})+C^{\beta}_{p}(T-T_{tr})-C^{\beta}_{p}T\ln(T/T_{tr}) \tag{14}$$

where μ_{tr} and s_{tr} are the chemical potential and molar entropy at T_{tr}, respectively. Since μ^{α}_{tr} equals μ^{β}_{tr}, the combination of Eq. 1, Eq. 13 and Eq. 14 gives the difference between μ^{α} and μ^{β}, which is denoted by $\Delta\mu$.

$$\Delta\mu=\mu^{\beta}-\mu^{\alpha}=\Delta_{tr}H(1-T/T_{tr})+\Delta C_{p}(T-T_{tr})-\Delta C_{p}T\ln(T/T_{tr}) \tag{15}$$

where $\Delta_{tr}H$ and ΔC_p are defined as follows.

$$\Delta_{tr}H\equiv H^{\beta}-H^{\alpha} \quad \text{at} \quad T=T_{tr} \quad \text{and} \quad \Delta C_{p}=C^{\beta}_{p}-C^{\alpha}_{p} \tag{16}$$

In spite of the definition of μ_{rel} in Eq. 11 with the constants referring to the k_1 phase, the value given by Eq. 15 is generally considered to be the same as the difference of μ_{rel} between α and β phases, regardless of the case that neither α nor β might represent k_1. Thus,

$$\mu^{\beta}-\mu^{\alpha}=\mu^{\beta}_{rel}-\mu^{\alpha}_{rel} \tag{17}$$

Now, substituting the corresponding quantities of the k_1/i transition, *i.e.* 29.0 kJ mol^{-1}, 0.21 kJ K^{-1} mol^{-1} and 321.2 K, for $\Delta_{tr}H$, ΔC_p and T_{tr} in Eq. 15, and taking into consideration Eq. 17, we plotted the μ_{rel} *vs.* T curve for the i phase on the basis of the curve for the k_1 phase in Fig. 4.

Analogously to the estimation of μ_{rel} from k_1 to i, we obtained the values of μ_{rel} for k_2 from i, for c from i and for s from c, by substituting into Eq. 15 the corresponding values of $\Delta_{tr}H$, ΔC_p and T_{tr} at the k_2/i, c/i and s/c transitions, *i.e.*, 27.0 kJ mol^{-1}, 0.20 kJ K^{-1} mol^{-1} and 317.4 K; 0.84 kJ mol^{-1}, -0.09 kJ K^{-1} mol^{-1} and 321.0 K; and 1.26 kJ mol^{-1}, 0.09 kJ K^{-1} mol^{-1} and 315.9 K, respectively.

From the inspection of Fig. 4 with reference to Chart 1, the following conclusions can be drawn for the various ChO phases, at least in the temperature range from 300 K to 330 K. (i) Thermodynamically, the k_1 phase is more stable than the k_2 phase. This is the reason for the transfer from k_2 to k_1 of ChO which was observed during storage as a relative increase of the higher melting form in crystalline ChO with two DSC peaks.[7] (ii) The observed phases, c, s and k_2 as well as i below $T_{tr}(k_1/i)$ are in metastable states. (iii) The transition from i to k_1 is hindered by a kinetic barrier to the nucleation of k_1 in i. The possible formation of k_1 by supercooling gives way to the reversible formation of c, which takes place at T_{tr}(c/i) slightly below $T_{tr}(k_1/i)$ and for which a kinetic barrier is virtually absent. The transfer to the thermodynamically stable k_1 phase from the other metastable phase occurs at a considerably low temperature, frequently *ca.* 20 K below $T_{tr}(k_1/i)$, usually after the transition from c to s, which takes place as easily as the i/c transition. (iv) Irreversibility of the transfer c/k_1 or s/k_1 is clear from the drop of chemical potential in Fig. 4. The changes of x_1 in Fig. 3 also indicate irreversible c/k_2 or s/k_2 transition occurring simultaneously with the c/k_1 or s/k_1 transition and reflect a relatively lower potential barrier from c or s to k_2 than to k_1. (v) On heating of ChO-T, the transition paths from k_2 to c to i cannot be ruled out, although they were not observed in the DSC thermograms, where the k_1/i transition obstructs the observation of possible c/i transition after k_2/c, and the characteristic tint of c phase was not observed by PM during the melting of ChO-T crystals. (vi) Clearly from Eq. 15, the differences of chemical potential between s and c as well as c and i are small due to the small $\Delta_{tr}H$ and ΔC_p, especially

the former. Therefore, it is probable that a trace amount of impurities is responsible for the differences of transition temperature among samples, as seen in Table II, in s/c and c/i more than in the k_1/i and k_2/i transitions.

In Situ Crystallization in the DSC Pan

Taking into consideration the above-mentioned findings that k_1 is thermodynamically more stable, but has a higher potential barrier than k_2 and also that time and temperature would help the stable state by providing a chance to jump over the kinetic barrier, we can predict that ChO crystals with higher x_1 are formed at higher temperature. This was confirmed by the results shown in Fig. 3 and also by the tendency for the DSC thermogram of ChO which was crystallized by rapid and deep freezing from solution to change on aging at room temperature from a single-peak (see Fig. 1(c)) appearing at lower temperature (k_2/i) to a double-peak showing the coexistence of k_1/i and k_2/i.

Unlike the above-mentioned crystallization, whose conditions can be easily regulated, the crystallization of ChO from i on cooling in a DSC pan, that is, *in situ* crystallization, usually involves supercooling and is difficult to control. When ChO samples from *in situ* crystallization are reheated, their DSC thermograms show variable patterns, mostly of the sort shown in Fig. 1, but sometimes with an exotherm between the peaks, as can be seen in Fig. 5(a). The exotherm observed in the sample from *in situ* crystallization was not found in the samples crystallized by cooling or solvent evaporation from solution. Therefore, the following conclusions may be reached concerning the ChO in DSC pans. The crystals in the k_1 and k_2 phases in the latter samples are independent of each other, resulting in the separate fusion of

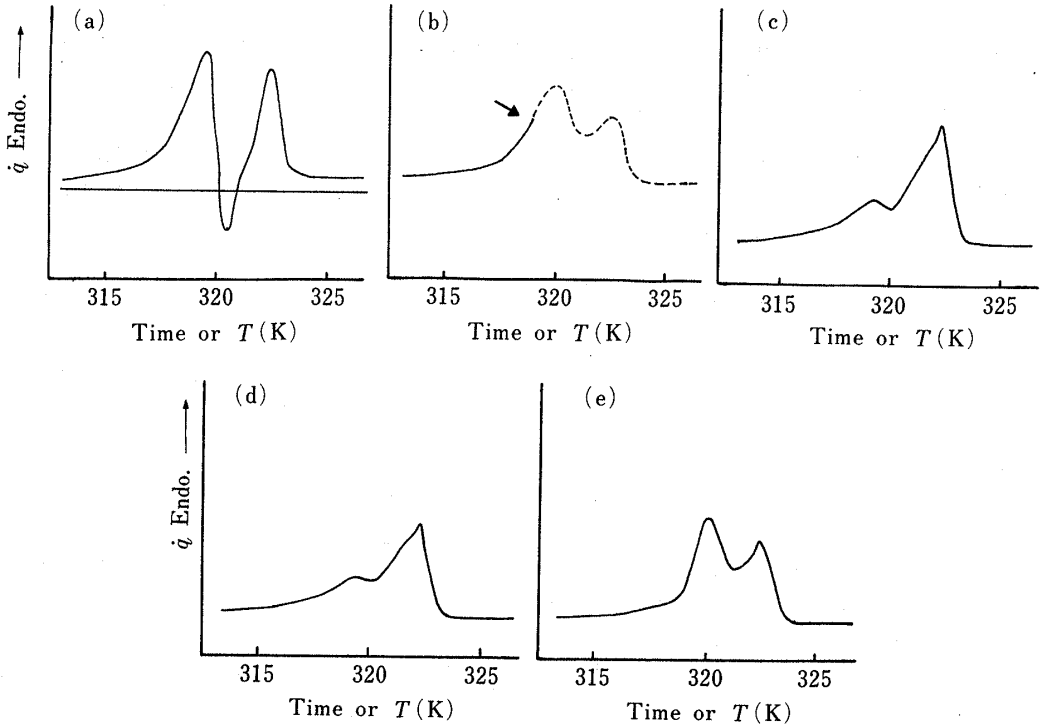

Fig. 5. DSC k/i Transition Thermograms of Cholesteryl Oleates Recrystallized *in Situ*

The ordinate and abscissa are the same as in Fig. 1. (a) Thermogram on reheating samples crystallized *in situ* through cooling at *ca.* 0.5 K min^{-1} from the melt or i phase to room temperature. (b) Solid curve: heating path of ChO-T on the DSC thermogram. At the prearranged temperature, which is indicated by an arrow, heating was stopped for annealing. The broken curve: hypothetical path, which would be followed in the absence of annealing. (c)—(e): Thermograms of *in situ*-crystallized samples. Holding time for annealing: 15 min. Maximum annealing temperature, T_M: 320.6 K (c), 320.4 K (d), 319.2 K (e).

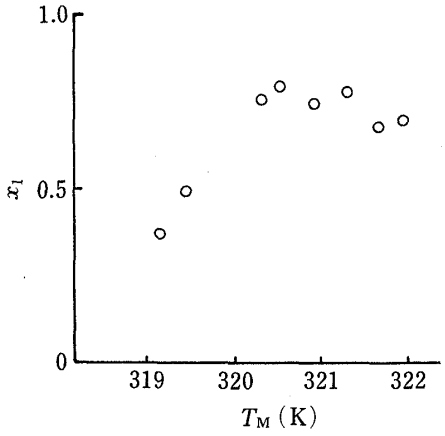

Fig. 6. The Mole Fraction of k_1 Phase; x_1, of Cholesteryl Oleate Crystallized *in Situ vs.* the Maximum Temperature for Annealing, T_M

both phases on heating. On the other hand, the exotherm in the former samples on heating suggests the occurrence of irreversible i/k_1 or c/k_1 transition, or in other words the growth of k_1 phase, which is induced by the presence of k_1 phase as a seed in the melt (i or c) of k_2 phase. The k_1 and k_2 phases probably coexist in a more intimate mixture in this case.

Now, taking account of the possible growth of k_1 phase in the DSC pan after k_2/i or k_2/c transition on heating, we stopped heating ChO samples at the point indicated by an arrow in Fig. 5(b) on the way to otherwise complete melting, as shown by the broken curve, and cooled them down after annealing for *ca.* 15 min between the maximum temperature, T_M, and 1 K below it. The exotherm indicating crystallization appears during the annealing and finishes shortly after it. The heating and cooling rates before and after annealing were 0.5 and 0.4 K min^{-1}, respectively. After cooling to room temperature, the samples were reheated for DSC thermograms, several examples of which are shown in Fig. 5(c), (d) and (e), from which the relation between x_1 and T_M in Fig. 6 was obtained. As expected, a k_1-rich ChO sample can be obtained by controlled *in situ* crystallization.

In conclusion, we were able to elucidate thermodynamically the transition paths and differences in stability between various phases of ChO on the basis of relative chemical potential from the results obtained by DSC. We could also partially control the crystallization of ChO, which yields two kinds of crystalline phases, under various conditions. We are currently studying various properties of ChO as well as other mesogenic cholesteryl esters.

Acknowledgement The authors are indebted to the Research Laboratory of Nippon Oil & Fats Co., Ltd. for the supply of cholesteryl oleate together with the information on its preparation.

References and Notes

1) For liquid-crystalline systems, we use the terminology proposed by Kelker and Hatz.[2a)]
2) *a*) H. Kelker and Hatz, "Handbook of Liquid Crystals," Chapt. 1, Microscopic Investigations Including Basic Concepts, Phenomenology, and Morphology, Verlag Chemie, Weinheim, 1980; *b*) *Ibid.*, Chapt. 12, Liquid Crystals in Living Systems.
3) I. Miyata and H. Kishimoto, *Yakugaku Zasshi*, **98**, 689 (1978).
4) I. Miyata and H. Kishimoto, *Yakugaku Zasshi*, **98**, 1629 (1978).
5) I. Miyata and H. Kishimoto, *Chem. Pharm. Bull.*, **27**, 1412 (1979).
6) I. Miyata and H. Kishimoto, *Chem. Pharm. Bull.*, **28**, 619 (1980).
7) R. J. Krzewki and R. S. Porter, *Mol. Cryst. Liq. Cryst.*, **21**, 99 (1973).
8) D. Armitage, *Phys. Lett.*, **65A**, 68 (1978).
9) G. J. Davis and R. S. Porter, *Mol. Cryst. Liq. Cryst.*, **6**, 377 (1970).
10) *a*) "Kagaku Benran, II," 3rd ed., ed. by Chem. Soc. Jpn., Maruzen, Tokyo, 1984, pp. 221—329; *b*) J. A. Dean (ed.), "Lange's Handbook of Chemistry," 12th ed., McGraw-Hill, New York, 1978.
11) D. Demus and L. Richter, "Textures of Liquid Crystals," Verlag Chemie, Weinheim, 1978.
12) G. R. Van Hecke, *J. Chem. Educ.*, **53**, 161 (1976).